Prediction of Resonance Frequency and Mode Shape of Rotor in Switched Reluctance Motor

Kyung-Ho Ha, Seung-Kyu Jeong, Jung-Pyo Hong and Do-Hyun Kang

Abstract - This paper investigates the influence of various stator pole shapes and yoke structures in Switched Reluctance Motors (SRM) on the mechanical behavior caused by the electromagnetic force. The stator part in SRM produces most vibration. The geometric design of the stator is therefore necessary to reduce the vibration. Based on electromagnetic and structural Finite Element Method (FEM), the free and forced vibrations for the various structures of SRM with 6/4 poles are analyzed. Then a less vibration stator structure is proposed. Some of numerical computations for a prototype motor are verified by experimental results.
Keywords - mode shape, resonance frequency, SRM and transfer matrix method.

1. Instruction

SRM is a fascinating machine with all kinds of interesting application possibility because it has many advantages such as the possibility of high-speed operation and simplicity of mechanical construction. However, the most striking disadvantages of the SRM are high levels of vibration and torque ripple. Among many possible sources of vibration and noise in SRM, the relationship between magnetic and mechanical origins is to be focused. The dominant sources are deformation of stator and eccentricity caused by rotor dynamics when the natural frequencies of the stator or rotor are close to the frequency of the electromagnetic force [1]. The mechanical origin for the magnetic force is classified into two parts, which are the stator and the rotor.

The commutation of the tangential forces, which are exerted on the poles of the stator and the rotor and produce torque, can excite vibration of the stator and rotor. In the aspects of the stator, normal SRM operation is characterized by radial forces on opposite poles, which tend to deform the stator into oval. The stator vibration mode will be excited when the radial forces on the stator poles coincide with the natural vibration [1], [2]. The modal deflection of the stator back iron as a ring can be predicted from calculating the modal analysis.

Especially, the rotor will get into resonance when it rotates at speeds equal to the bending natural frequency and these speeds are called as critical speeds or resonance speeds [3]. Moreover, the determination of the position of bearing on the shaft, bearing stiffness and balancing technology are principally associated with rotor vibration mode. It is therefore necessary to know the natural frequencies and vibration modes of the rotor as well. These should be investigated at the design stage. The existing research on vibration mode and acoustic noise of the SRM mostly deals with the stator part of motor [1]-[6]. This paper deals with the rotor behavior to avoid resonance speed in high-speed operation.

In order to determine the critical speeds and modes, a suitable analysis method is required to reduce calculation time. A Finite Element Method (FEM) is well established for structural analysis of the motor. Its inherent drawbacks, however, are its complexity and the length of time. It takes a lot of time to obtain a solution because the matrix size depends on the number of elements and the Degree of Freedom (DOF) at each node. On the other side, the Transfer Matrix Method (TMM) is independent of the number of element, so it can have the fixed matrix size regardless of the number of element and reduce the computing time. In this paper, the rotor is modeled as several lumped masses connected by massless elastic shaft.

Based on the structural TMM and elasticity theory, 3-dimensional vibration modes and resonant frequencies of rotor-bearing system for SRM are analyzed and demonstrated in this paper. The analysis results are validated by measurements and then the computational gain of the proposed method is compared with that of 3-D FEM.

2. Analysis Model

The analysis model of SRM has 4 rotor poles and 6 stator poles with three phases winding in the stator. Table I presents the main specifications and the measured mechanical properties needed for analysis of mechanical structure. Fig.1 shows the configuration of the rotor and the analysis model. The analysis model of the rotor supported on bearings is divided into several lumped masses and then

Manuscript received: Nov. 5, 2001 accepted: Jan. 14, 2002.

Kyung-Ho Ha and Seung-Kyu Jeong are presently pursuing the Ph. D. degree in the Department of Electrical Engineering at Changwon National University, Changwon, Kyungnam, 641-773, Korea.

Jung-Pyo Hong is with the Department of Electrical Engineering at Changwon National University, Changwon, 641-773, Kyungnam, Korea.

Do-Hyun Kang is with the Mechatronics Research Group of Korea Electrotechnology Research Institute.

they are constructed by connecting the nth lumped mass as massless elastic shaft.

Table 1 Specification of Analysis Model and Material Property

Item	Value	Item	Value
Rotor core mass density	7850 (kg/m^3)	Shaft mass density	7900 (kg/m^3)
Bearing stiffness	5.36×10^5(N/m)	Young's Modulus	205 (Gpa)

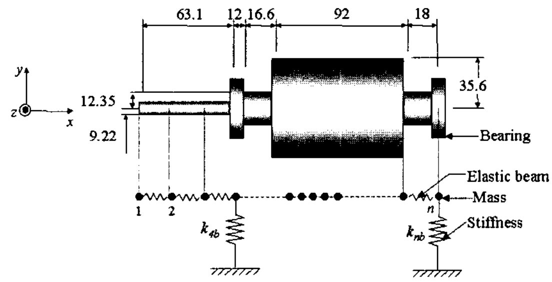

Fig. 1 Configuration and analysis model of lumped mass

3. Analysis Method

A. Transfer matrix method [3]

The form of the point matrix $[\mathbf{P}]_i$, representing the mathematical expression of the lumped masses, is derived from equilibrium relation for the mass at the ith point. The field matrix $[\mathbf{F}]_i$, representing the massless elastic shaft, is derived from the solution of the governing differential equation of a uniform beam. The point and field matrixes for the 3-D analysis model each have eight DOF. The 8 by 8 overall transfer matrix from *1* to *n*th station in the over all system is developed from the product of all field and point matrix in series. The modal analysis is obtained by solving the overall transfer matrix.

The state vector {S} that presents DOF in each element is composed of deflection ω_y and ω_z, angle deflection θ_y and θ_z, bending moment M_z and M_y, shear forces V_y and V_z in the x-y and x-z planes.

From the equilibrium relation for the mass at point i, as shown in Fig 2, we can directly write the following point transfer matrix.

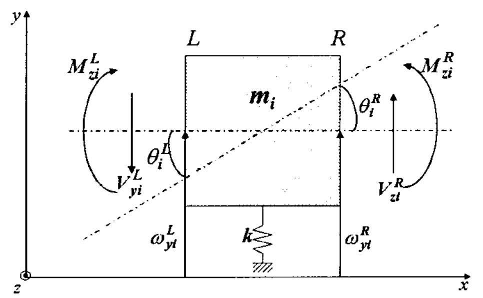

Fig. 2 Equilibrium relations for *i*th mass in x-y plane

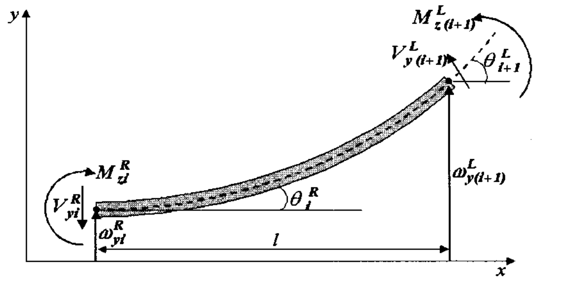

Fig. 3 Relations for *i*th massless elastic shaft in x-y plane

$$\{\mathbf{S}\}_i^R = [\mathbf{P}]_i \{\mathbf{S}\}_i^L$$

$$[\mathbf{P}]_i = \begin{bmatrix} 1 & 0 & 0 & 0 & 0 & 0 & 0 & 0 \\ 0 & 1 & 0 & 0 & 0 & 0 & 0 & 0 \\ 0 & 0 & 1 & 0 & 0 & 0 & 0 & 0 \\ 0 & 0 & 0 & 1 & 0 & 0 & 0 & 0 \\ m\lambda^2 + K_{yy} & K_{yz} & 0 & 0 & 1 & 0 & 0 & 0 \\ K_{zy} & m\lambda^2 + K_{zz} & 0 & 0 & 0 & 1 & 0 & 0 \\ 0 & 0 & -I_p\lambda^2 & I_t\lambda^2 & 0 & 0 & 1 & 0 \\ 0 & 0 & I_t\lambda^2 & -I_p\lambda^2 & 0 & 0 & 0 & 1 \end{bmatrix} \quad (1)$$

where {S}i is state vector, [P]i is the point matrix for ith mass vibrating in a normal mode with frequency λ, m is mass and K is stiffness of bearing. Ip and It is pole inertia moment and transverse moment, respectively.

The solution of the governing differential equations of an uniform beam segment connecting *i*th mass from differential equation of elastic curve and area moment method, as shown in Fig.3, are written in a transfer matrix as

$$\{\mathbf{S}\}_{i+1}^L = [\mathbf{F}]_i \{\mathbf{S}\}_i^R$$

$$[\mathbf{F}]_i = \begin{bmatrix} 1 & 0 & 0 & L & L/GAk_s - L^3/6EI & 0 & L^2/2EI & 0 \\ 0 & 1 & 0 & 0 & 0 & L/GAk_s - L^3/6EI & 0 & L^2/2EI \\ 0 & 0 & 1 & 0 & 0 & L^2/2EI & 0 & L/EI \\ 0 & 0 & 0 & 1 & -L^2/EI & 0 & L/EI & 0 \\ 0 & 0 & 0 & 0 & 1 & 0 & 0 & 0 \\ 0 & 0 & 0 & 0 & 1 & 1 & 0 & 0 \\ 0 & 0 & 0 & 0 & -L & 0 & 1 & 0 \\ 0 & 0 & 0 & 0 & 0 & L & 0 & 1 \end{bmatrix} \quad (2)$$

where $[\mathbf{F}_i]$ is the field matrix for the *i*th massless elastic shaft and E is the Young's modulus. I is inertia of moment and L is the length between the lumped mass.

The 8 by 8 overall transfer matrix [T] from station 1 to *n*th station in the over all system is constructed by the product of all field and point matrices in series. It can be written as

$$\{\mathbf{S}\}_n^R = [\mathbf{P}]_n[\mathbf{F}]_{n-1}[\mathbf{P}]_{n-1}\cdots\cdots[\mathbf{P}]_2[\mathbf{F}]_1[\mathbf{P}]_1\{\mathbf{S}\}_1^L = [\mathbf{T}]\{\mathbf{S}\}_1^L$$

$$\begin{Bmatrix} \omega_y \\ \omega_z \\ \theta_y \\ \theta_z \\ V_y \\ V_z \\ M_y \\ M_z \end{Bmatrix}_n^R = \begin{bmatrix} T_{11} & T_{12} & T_{13} & \cdot & \cdot & \cdot & \cdot & T_{18} \\ T_{21} & \cdot & & & & & & \\ T_{31} & & \cdot & & & & & \\ \cdot & & & \cdot & & & & \\ \cdot & & & & \cdot & & & \\ \cdot & & & & & \cdot & & \\ \cdot & & & & & & \cdot & \\ T_{81} & & & & & & & T_{88} \end{bmatrix} \begin{Bmatrix} \omega_y \\ \omega_z \\ \theta_y \\ \theta_z \\ V_y \\ V_z \\ M_y \\ M_z \end{Bmatrix}_1^L \quad (3)$$

An algebraic equation is obtained by imposing the free boundary condition in equation (3); V=0, M=0 at both lumped mass 1 and nth. The solution of the eigenvalue equation can be obtained by a root-finding technique for the value of λ. Once the natural frequency is found, the corresponding mode shape can be determined by unit slope ω_0 =1at the first mass.

B. Structural finite element analysis

The vibration equation for a mechanical undamped system based on the principle of Hamilton can be expressed in matrix notation when the free vibration is periodic [5]:

$$([\boldsymbol{K}]-\lambda^2[\boldsymbol{M}])\{\boldsymbol{\phi}\}=\{0\} \tag{4}$$

where eigenvector $\{\phi\}$ presents the mode shape at the natural angular velocity, $[\boldsymbol{M}]$ and $[\boldsymbol{K}]$ are the global mass matrix and stiffness matrix, respectively. The above equation has a nonzero solution. From the roots of the determinant in the parenthesis of equation (4), the natural frequencies and modes of rotor can be determined.

4. Computation and Measurement Results

In TMM, the model is divided into 28 lumped masses and then they are constructed by connecting the each mass as an uniform beam segment. For FEM using ANSYS, about 2606 hexahedron-shaped elements are used for 3-D modeling of solid structure that is defined by eight nodes having three DOF at each node. Fig. 4 shows the mesh generation result of analysis model for 3-D FEM. The computation for solving the natural frequencies is implemented with the aid of a Pentium Celeron433 computer.

Fig. 5 shows the measured frequency response function obtained from the experimental modal analysis. The inertance in the y-axis is the transfer function resulting from the relationship between impulsive excitation and acceleration signal. The natural frequencies exist within the audible sound range. In this experimental modal analysis, the frequency response function is measured by an impact test. The modal system consists of accelerometer, spectrum analyzer and stationary rotor. The accelerometer is attached to the rotor body.

Table 2 shows the comparison of calculation and measurement for the natural frequencies of the rotor. The analysis results obtained by FEM and TMM are in good agreement with the experimental values. The computational error is mainly attributed to the simplicity of the computing model. The amplitude 4th natural frequency is greater than that of the other mode and it is due to the lamination along the stack length.

Table 3 shows the computation gain and the computing time in each analysis method. The computation gain is defined as the proportion of computing time using FEM to using TMM. The method of TMM can reduce the computing time by about six times that of FEM.

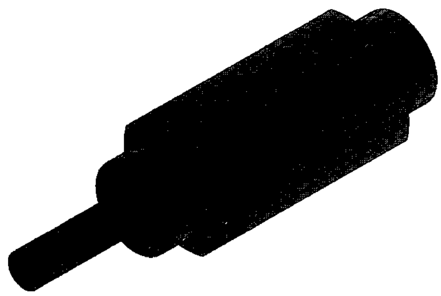

Fig. 4 Analysis model with hexahedron-shaped elements for 3-D FEM

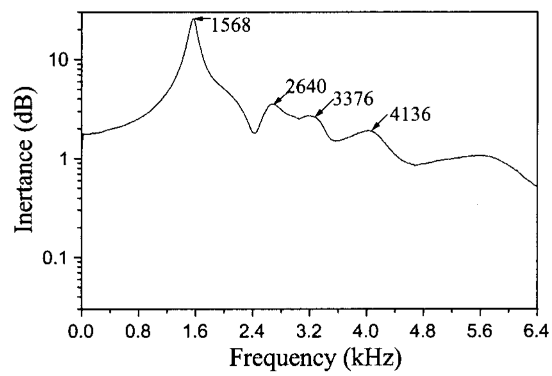

Fig. 5 Analysis model with hexahedron-shaped elements for 3-D FEM

Table 2 Natural Frequency Comparison

Mode	TMM(Hz)		FEM(Hz)		Measured frequency
	Freq.	Error	Freq.	Error	
1st	1588	1.28	1578	0.64	1568
2nd	2812	6.52	2535	3.98	2640
3rd	3501	3.70	3327	1.45	3376
4th	4532	9.57	4686	13.30	4136

Table 3 Computation Gain and Node Number Comparison

Item	No. of node	Computing time (sec)	Computation gain (FEM/TMM)	Average Error for experiment
TMM	28	40	1	5.02
FEM	2606	263	6.6	4.84

Fig. 6 shows the mode shapes for the rotor corresponding to the natural frequencies in 2-D plane. The displacement value of mode shape displayed in Fig. 6 is normalized. The calculations are based on a 3-D TMM structural analysis considering the bearing of rotor. The 2nd and 3rd modes have one and two nodal points, respectively. If rotor bearings are placed in these nodal points, the vibration tends to be increased. Therefore, the bearing position should avoid these nodal points.

Each rotor behavior that corresponds to a resonant frequency is displayed on 3D spatial plane is shown in Fig. 7. These mode shapes present the locus of rotor center along stack length when the rotor is rotating. There are two whirling modes of a rigid rotor in flexible end bearings. Fig. 7(a) is the translatory whirling motion and Fig. 7(b) is the conical whirling motion of rotor. The first and second modes do not produce deformation of rotor along the shaft elastic axis, because the behavior of rigid body rotor is caused by the stiffness of the rotor bearing supporting both end of rotor. These two modes become the origin that produces the eccentricity of rotor in an electric machine. In order to reduce vibration in these modes, it is important to select the bearing with appropriate stiffness based on the modal analysis.

An accurate analysis of resonant frequencies and the rotor design can be achieved from proposed analysis method. In addition, the analysis about modal analysis will allow us to propose a less noisy structure and resonant speed.

5. Conclusion

This paper presents a method to calculate the natural frequencies and their mode shapes of the rotor in SRM. Transfer matrix method is used to reduce the calculation time. The validation of the proposed method is verified by comparing its calculation results with the experimental one. In addition, the effect of the three dimensional mode shapes of rotor on the vibration characteristic is investigated and described. Due to the reduction of the computation, the method proposed in this paper is more practical for estimation of the natural frequencies of the rotor and regulating the designing scheme in designing the rotor of SRM for high speed.

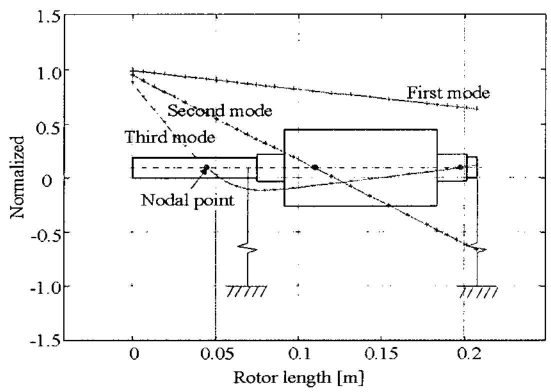

Fig. 6 Mode shapes of the SRM rotor in two-dimensional plane

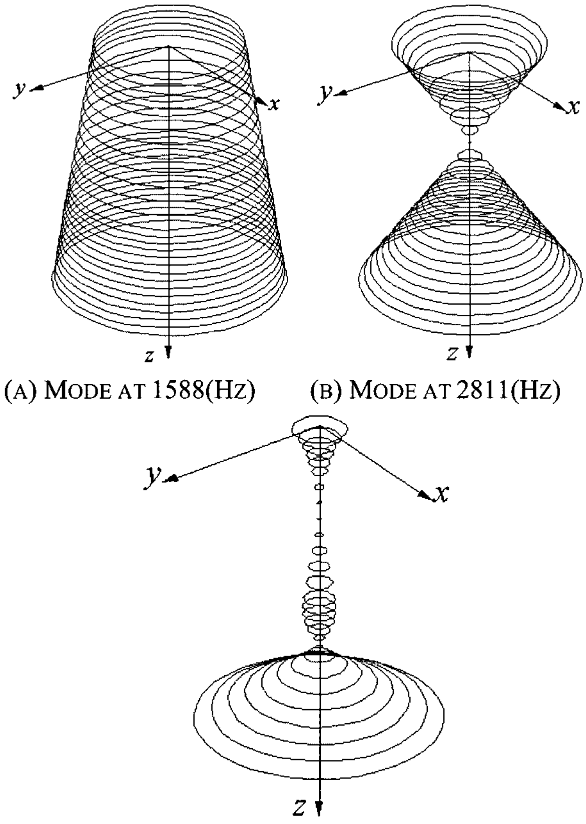

(A) MODE AT 1588(HZ) (B) MODE AT 2811(HZ)

(c) Mode at 3501 Hz

Fig. 7 3-D whirling mode with corresponding to natural frequency of rotor

References

[1] C. Picod, M. Besbes, Camus and M. Gabsi, "Influence of stator geometry upon vibratory behaviour and electromagnetic performance of switched reluctance motors," *IEE Proceeding of Electric Power Application*, vol. 145, pp. 462-468. 1998.

[2] R. S. Colby, F. M. Mottier and T. J. E. Miller, "Vibration modes and acoustic noise in a four-phase switched reluctance motor," *IEEE Transaction on Industry Application*, vol. 32, pp. 1357-1364, 1996.

[3] J. S. Rao, *Rotor Dynamics*, John Wiley & Sons, 1991.

[4] C. G. C. Neves *et al.*, " Vibration behavior of switched reluctance motors by simulation and experimental procedures," *IEEE Transaction on Magnetics*, vol. 34, pp. 3158-3136, 1998.

[5] P. Pillay and W. Cai, "An investigation into vibration in switched reluctance motors," *IEEE Trans. Industry Application*, vol. 353, pp. 589-596. 1999.

[6] C. Yongxiao, W. Jianhua and H Jun, "Analysis calculation of natural frequencies of stator of switched reluctance motor," *IEE EMD97*, pp. 81-84. 1997.

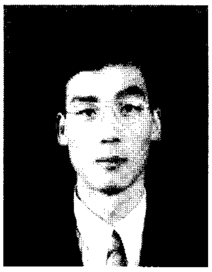

Kyung-Ho Ha was born in 1972. He received the B.S. and M.S. Degrees from Changwon National University, Changwon, Korea. He is presently pursuing the Ph.D. degree in Dept. of Electrical Engineering at Changwon National University. His research interest includes design of electric machine, numerical analysis of electromagnetic and motor vibration.

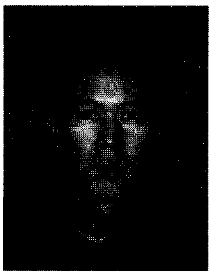

Seung-Kyu Jeong was born in 1964. He received the B.S. and M.S. Degrees from Pusan National University, Pusan, Korea. He worked as a senior researcher engineering of Digital Appliance Research Lab. at LG Electronics Inc. until 1999. He is presently pursuing the Ph.D. degree in Dept. of Electrical Engineering at Changwon National University and has been work as a manager at EM-Tech. His research interests include design of electric machine, numerical analysis of electromagnetic and motor vibration.

Jung-Pyo Hong was born in 1959. He received the B.S., M.S. and Ph.D. degrees from Hanyang University, Seoul, Korea. Between 1992 and 1995, he was employed by LG Precision Co., Ltd. as an associate research engineer. Between 1990 and 1992, he was employed by Samsung Electric Co., Ltd as a senior research engineer. Since 1996, he has been an assistant processor in the Department of Electrical Engineering at Changwon National University, Changwon, Korea. His research interests are design of electrical machine, optimization, coupled problem and numerical analysis of electromagnetic.

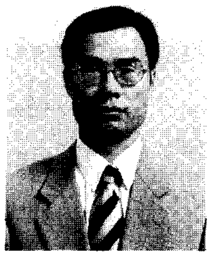

Do-Hyun Kang was born in Busan, Rep. of Korea in 1958. He received B. S. Degree in 1981 and M. S. Degree in 1989 in Electrical Engineering from the Hanyang University, Seoul, Korea and the Ph.D. degree in 1996 in Institute of Electric Machines, Traction and Drives from Technical University Braunschweig, Braunschweig, Germany. He worked as a design engineer in Nuclear Power Plant at Hyundai Construction Co. from 1981 until 1986. He is the director of Mechatronics Research Group of Korea Electrotechnology Research Institute. His research interests are magnetic levitation, linear drives and new electric machines.